JOURNAL OF GEOPHYSICAL RESEARCH, VOL. 114, D06108, doi:10.1029/2008JD011333, 2009

Short-term production and synoptic influences on atmospheric ^{7}Be concentrations

Ilya G. Usoskin,[1] Christy V. Field,[2] Gavin A. Schmidt,[2] Ari-Pekka Leppänen,[3] Ala Aldahan,[4,5] Gennady A. Kovaltsov,[6] Göran Possnert,[7] and R. Kurt Ungar[8]

Received 21 October 2008; revised 8 January 2009; accepted 21 January 2009; published 21 March 2009.

[1] Variations of the cosmogenic radionuclide ^{7}Be in the global atmosphere are driven by cooperation of processes of its production, air transports, and removal. We use a combination of the Goddard Institute for Space Studies ModelE and the OuluCRAC:7Be production model to simulate the variations in the ^{7}Be concentration in the atmosphere for the period from 1 January to 28 February 2005. This period features significant synoptic variability at multiple monitoring stations around the globe and spans an extreme solar energetic particle (SEP) event that occurred on 20 January. Using nudging from observed horizontal winds, the model correctly reproduces the overall level of the measured ^{7}Be concentration near ground and a great deal of the synoptic variability at timescales of 4 days and longer. This verifies the combined model of production and transport of the ^{7}Be radionuclide in the atmosphere. The impact of an extreme SEP event of January 2005 is seen dramatically in polar stratospheric ^{7}Be concentration but is small near the surface (about 2%) and indistinguishable given the amount of intrinsic variability and the uncertainties of the surface observations.

Citation: Usoskin, I. G., C. V. Field, G. A. Schmidt, A.-P. Leppänen, A. Aldahan, G. A. Kovaltsov, G. Possnert, and R. K. Ungar (2009), Short-term production and synoptic influences on atmospheric ^{7}Be concentrations, *J. Geophys. Res.*, *114*, D06108, doi:10.1029/2008JD011333.

1. Introduction

[2] As modern atmospheric air transport models achieve higher level of sophistication, their testing and evaluation becomes increasingly important (see, e.g., section 8.1.2 of *IPCC* [2007]). Testing of air transport models can be done by measuring the concentration of tracing substances with known sources and comparing them with model predictions. Atmospheric dynamics in the troposphere can be tested in this way using anthropogenic (radioactive, e.g., the Chernobyl accident, or chemical) or natural (e.g., volcanic eruptions) traceable pollutant emissions. The tracing method is more difficult to apply for the stratosphere [e.g., *Rind et al.*, 1999]. Here we present a new quantitative method to probe the atmospheric dynamics using the short-lived cosmogenic isotope ^{7}Be as a tracer of air mass. Since it is produced mainly at midlatitude and high latitudes and mostly in the stratosphere, this tracer appears useful for looking at stratosphere-troposphere exchange and also for horizontal transport, and it can also be used as a tracer for aerosol removal processes. The potential usefulness of this cosmogenic tracer was first highlighted long time ago [e.g., *Lal and Peters*, 1962; *Raisbeck et al.*, 1981; *Koch and Rind*, 1998] but now its potential can be explored to much greater extent. The method of cosmogenic tracers is applicable for all locations and times, particularly at high latitudes [*Koch and Rind*, 1998; *Aldahan et al.*, 2001; *Jordan et al.*, 2003; *Koch et al.*, 2006].

[3] Cosmic rays, which are highly energetic nucleons (mostly protons and α particles) of extraterrestrial origin, continuously bombard the Earth's atmosphere, resulting in various physical and chemical effects [see, e.g., *Dorman*, 2004]. In particular, quite a number of different radioactive isotopes are produced as a by-product of nucleonic-electromagnetic cascades initiated by cosmic rays in the atmosphere. One of them is the short-lived radionuclide ^{7}Be (half-life $T_{1/2} \approx 53.22$ days), which is a product of spallation of atmospheric O and N nuclei caused by the nucleonic component of the cosmic ray-induced atmospheric cascade. An important advantage of this nuclide is that its concentration in the ambient air is easy to measure (see section 2.1). Accordingly, data on routine ^{7}Be measurements near the ground (typically with weekly resolution) have been performed at different stations around the world for the last several decades, in the framework of radiation safety

[1] Sodankylä Geophysical Observatory (Oulu unit), University of Oulu, Oulu, Finland.
[2] NASA Goddard Institute for Space Studies, New York, New York, USA.
[3] Regional Laboratory in Northern Finland, STUK (Radiation and Nuclear Safety Authority), Rovaniemi, Finland.
[4] Department of Earth Sciences, University of Uppsala, Uppsala, Sweden.
[5] Department of Geology, United Arab Emirates University, Al Ain, United Arab Emirates.
[6] Ioffe Physical-Technical Institute, St. Petersburg, Russia.
[7] Tandem Laboratory, University of Uppsala, Uppsala, Sweden.
[8] Radiation Protection Bureau of Health Canada, Ottawa, Ontario, Canada.

0148-0227/09/2008JD011333$09.00

Table 1. ^{7}Be Measuring Sites Used in This Study

Code	Location	Coordinates
	Northern hemisphere	
SEP63	Stockholm (Sweden)	59.38°N 17.95°E
HEL	Helsinki (Finland)	60.21°N 25.05°E
CAP15	Resolute (Canada)	74.71°N 95.0°W
CAP16	Yellowknife (Canada)	62.47°N 114.47°W
DEP33	Freiburg[a] (Germany)	47.9°N 7.9°E
USP72	Melbourne (Florida, USA)	28.1°N 80.6°W
	Southern hemisphere	
AUP04	Melbourne (Australia)	37.7°S 145.1°E
AUP09	Darwin (Australia)	12.43°S 130.9°E
AUP10	Perth (Australia)	31.9°S 116.0°E
NZP46	Chatham Island (New Zealand)	43.82°S 176.5°W
NZP47	Kaitaia (New Zealand)	35.07°S 173.3°E

[a]Elevation 1208 m a.s.l.

monitoring and emergency preparedness. It is important to note that cosmic rays are the only natural source of the isotope in the absence of anthropogenic nuclear accidents whose detection is the main purpose of the worldwide monitoring. Atoms of ^{7}Be become quickly attached to atmospheric aerosols, picked up by air masses and thus can trace them. The isotope's lifetime is, on the one hand long enough to allow for long-distance transport (both horizontally and vertically), and on the other hand short enough to prevent long-term accumulation of the isotope in large reservoirs (which would lead to a complicated global cycle). Accordingly, the isotope's transport is quite straightforward and provides a good opportunity to examine the dynamics of air masses on the timescale of days to months [e.g., *Koch et al.*, 1996; *Liu et al.*, 2001; *Jordan et al.*, 2003; *Yoshimori*, 2005a; *Kulan et al.*, 2006]. However, insufficient knowledge of the details about the isotope's production and transport, in particular the lack of a quantitative reliable production model, had limited earlier works to correlative studies and use of the isotopic ratio ^{7}Be/^{10}Be. An appropriate model with special emphasis on the production of ^{7}Be by cosmic rays in the atmosphere has recently been developed: the OuluCRAC:7Be (Cosmic Ray induced Atmospheric Cascade) model [*Usoskin and Kovaltsov*, 2008]. This model makes it possible to numerically simulate the full details of the isotope's production in the low and middle atmosphere. Now the output of the 3D (geographical coordinates, altitude) and time ^{7}Be production model can be used as an input for an atmospheric circulation model, which can predict the expected concentration of ^{7}Be in air at any location and time. These predicted concentrations can be directly compared with the isotope measurements performed regularly in different sites around the world.

[4] While galactic cosmic rays (GCR) are always present in the Earth's environment, additional sporadic fluxes of solar energetic particles (SEP) can occur due to solar eruptive phenomena (solar flares or coronal mass ejections), leading to transient changes in the ^{7}Be production. A severe SEP event, one of the strongest ever observed [*Plainaki et al.*, 2007], occurred during the period under investigation, on 20 January 2005 leading also to an observable atmospheric response [*Mironova et al.*, 2008]. According to the model computations [*Usoskin and Kovaltsov*, 2008], production of ^{7}Be was greatly enhanced in polar/subpolar regions (geomagnetic latitude above 60) in the entire atmospheric column during that day without any significant effect in the following days. Therefore a strong instantaneous "injection" of ^{7}Be trace atoms took place in a limited geographical area leading to a potentially observable effect in the measured ^{7}Be concentration.

[5] In this paper we perform such a comparison using the OuluCRAC:7Be model of ^{7}Be production, the Goddard Institute for Space Studies (GISS) ModelE atmospheric general circulation model (GCM) [*Schmidt et al.*, 2006] and a series of daily measurements of the ^{7}Be concentration in near-surface air at different sites. For the detailed analysis we have chosen the period of January to February 2005, which includes the SEP event mentioned above. The studied period corresponds to the middle of boreal winter/austral summer. Six ^{7}Be monitoring stations in the Northern hemisphere and five in the Southern hemisphere (see Table 1), ranging from the tropics to the polar region, provided daily data during the period under investigation.

2. Models and Data

2.1. Measurement

[6] The ^{7}Be measurements used here have been collected by sampling stations of the International Monitoring System (IMS) of the Comprehensive Nuclear Test Ban Treaty Organization (CTBTO). Additionally one station (HEL) from the Finnish national radiation monitoring system was used. The experimental data from the IMS are collected by the CTBTO in an international data center in Vienna, Austria [*Bratt*, 2001]. All the participating national organizations have access, via national data centers, to the raw measurement data recorded at every other station around the world. The IMS data used in this study has been obtained via the Finnish National Data Centre (FiNDC) at the Finnish Radiation and Nuclear Safety Authority (STUK). FiNDC and the Finnish radiation monitoring system analyzes the data using Unisampo and Shaman software in almost identical automated analysis pipelines, feeding LINSSI (Linux System for Spectral Information) databases [*Ungar et al.*, 2007; *Aarnio et al.*, 2008; *Ala-Heikkilä*, 2008]. Every measured spectra in the LINSSI database is analyzed in the same way thus ensuring that the analysis method does not cause any uncertainty between the results from different stations. The only station-to-station uncertainty in the final results comes from sampling and measurement procedure. For all the data used in this study, the necessary permissions to use the data have been obtained from the corresponding national authorities in the countries hosting the IMS stations.

[7] Concentration of ^{7}Be is measured in aerosol samples routinely collected at each station, using a high volume collector. Aerosols are captured by microfiber glass filters (pore size 1–2 μm) with very high retention capability (about 98% of the aerosol particles are captured). While the type and manufacturer of the sampler may vary between individual stations, they all fulfill the same basic requirements necessary for each station [*Mathews and Schulze*, 2001; *Medici*, 2001]. During the collection of the sample, air is pumped through a fiberglass filter where the aerosols are captured. The sampling volumes may vary between 15,000 and 25,000 m^{3} of air per collected sample. The air volume is measured with a flange and pressure gauges where measured air volume is affected by air pressure and

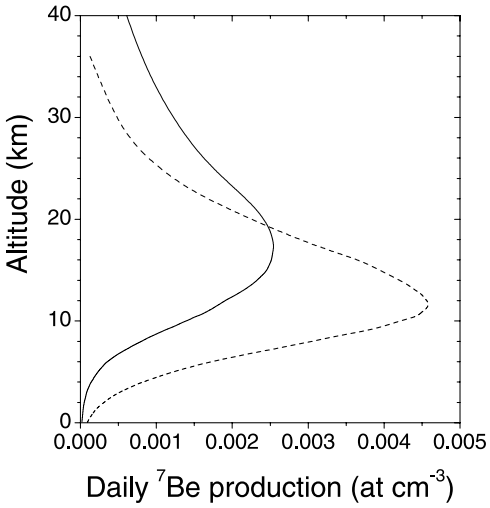

Figure 1. Daily production of ^{7}Be in a high-latitude region ($P_c = 2$ GV) as a function of altitude: solid curve indicates the effect of the SEP event of 20 January 2005; dotted curve indicates GCR for a quiet day of 12 January 2005.

moisture. The requirement for air volume uncertainty for the CTBTO IMS stations is ±5% [*Medici*, 2001]. The uncertainty varies between station types, for example, the uncertainty of air volume measurement at HEL station is ±2.5% (Lehtinen J., Senya Oy, personal communication, 2008). The sampling cycle is divided into three periods – collection, cooling down and measurement, with each period lasting 24 hours. The measurements of ^{7}Be concentration are performed by means of the γ-ray spectroscopy of the collected samples. The spectrum contains a strong line at 477.59 keV, corresponding to the decay of ^{7}Be. The photo efficiency of the line corresponds to the decay rate of ^{7}Be in the sample, and finally the ^{7}Be activity, typically quantified in μBq/m^3, is computed from the intensity of the 477.59 keV line. Measurements are performed with a HPGe detector to obtain a high resolution γ-ray spectrum. The detectors are calibrated via standard mixed radionuclide solution or by semi-empirical simulations. The systematic uncertainty caused by the detector calibration is generally around 3%. The measurement geometries, detector types, models and detector efficiencies vary from station to station, and the homogenous quality of data is ensured through intercomparison measurements. When all the uncertainties are taken into account, the total uncertainty for the measured ^{7}Be concentration is approximately 7–8%.

2.2. ^{7}Be Production Model

[8] The OuluCRAC:7BE model is based on detailed Monte-Carlo simulations, using CORSIKA [*Heck et al.*, 1998] and FLUKA [*Fassò et al.*, 2001] numerical packages, of the nucleonic-muon-electromagnetic cascade initiated by cosmic rays in the Earth's atmosphere. All the details of the model can be found elsewhere [*Usoskin and Kovaltsov*, 2008]. The 3D×time production rate Q of ^{7}Be in the atmosphere can be computed as a function of the altitude h, geographical longitude λ, latitude ψ, and time t as

$$Q(h,\lambda,\psi,t) = \int_{E_c(\lambda,\psi)}^{\infty} Y(h,E)\cdot S(t,E)\cdot dE, \qquad (1)$$

where $Y(h, E)$ is the ^{7}Be yield function at altitude h, provided by the OuluCRAC:7Be model; $S(t, E)$ is the differential energy spectrum of cosmic rays on the Earth's orbit outside the geomagnetosphere; and integration is over the kinetic energy E of primary cosmic rays above the energy E_c corresponding to the local geomagnetic cutoff. The model can deal with both galactic cosmic rays, which are always present in the near-Earth space, and transient SEP events, via applying the appropriate energy spectrum S in the equation. The digital tables of the ^{7}Be yield function are available from [*Usoskin and Kovaltsov*, 2008]. We used the force-field approximation of the galactic cosmic ray spectrum (see full details in the study by *Usoskin et al.* [2005]). The solar modulation potential (*Usoskin et al.* [2005], see http://cosmicrays.oulu.fi/phi) was taken for January and February 2005, and we include the additional ^{7}Be produced as a result of the severe SEP event on 20 January 2005. The spectrum of SEP for the event of 20 January 2005, was taken using the Ellison-Ramaty spectral form [*Ellison and Ramaty*, 1985], which is often used as a handy approximation for strong SEP events [e.g., *Lockwood et al.*, 1990; *Stoker*, 1995]. The SEP spectrum is the same as in the previous work (see Figure 4 in the study by *Usoskin and Kovaltsov* [2008]), and is obtained by fitting satellite data [*Mewaldt*, 2006] and ground based neutron monitor measurements. This computed production of ^{7}Be atoms was then used as an input for the atmospheric circulation model. The daily production of ^{7}Be was simulated for all altitudes and all grid boxes as described above using the parameters of the geomagnetic field from the IGRF-10 (tenth generation of the International Geomagnetic Reference Field, http://modelweb.gsfc.nasa.gov/magnetos/igrf.html) model for the epoch 2005. An example of altitude profile of ^{7}Be production is shown in Figure 1 for GCR and SEP. One can see that the maximum production of ^{7}Be due to GCR corresponds to the altitude of 12–15 km. Contribution from SEP becomes important at higher altitudes because of their greater flux but softer energy spectrum.

[9] Since we are primarily interested in the near-ground ^{7}Be concentration measurements, we consider primary particles with energy above 50 MeV/nucleon.

2.3. Atmospheric General Circulation Model

[10] Our simulations of the air mass transport were performed using the latest stratospheric version of GISS ModelE [*Schmidt et al.*, 2006]. The model top is at 0.002 mb atmospheric pressure, which is important for capturing the full range of stratospheric ^{7}Be production and also for providing a realistic depiction of transport between the stratosphere and the troposphere [*Rind et al.*, 1999, 2007; *Shindell et al.*, 2006]. Previous studies with ModelE have demonstrated its skill in simulating a variety of climatological features, and also in realistically simulating ^{7}Be [*Koch et al.*, 2006; *Field et al.*, 2006; *Schmidt et al.*, 2006]. We also note that the ^{7}Be production scheme used in these simulation, which allows for daily varying production and radioactive decay, is slightly improved with respect to our earlier model [*Field et al.*, 2006] in terms of how the production is partitioned over the vertical pressure levels. Local pressure variations can change the distribution with height of the ^{7}Be production: when local surface pressure is

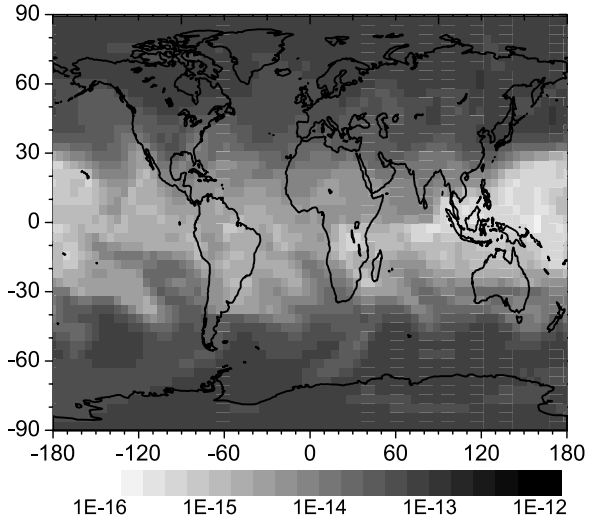

Figure 2. An example of the distribution of the computed ^{7}Be concentration (values in ppmv are given in the bottom gray scale) at the atmospheric level of 192 mb for quiet day of 12 January 2005.

higher (more mass), the ^{7}Be production occurs higher in the column. This was not accounted for in previous versions of the model. However, it makes only a minor difference to the tropospheric ^{7}Be concentrations since they are dominated by advection and mixing rather than by local production. Note that the decay of ^{7}Be is straightforwardly accounted in the model and the 53-day half-life is considerably longer than the weekly and monthly time series against which we compare our model output, therefore it does not affect our results.

[11] When simulating the ^{7}Be transport, we assume that there are always sufficient sulfate aerosols available to scavenge the ^{7}Be atoms, and that ^{7}Be attaches to sulfate aerosols immediately after production. We also assume that the sulfate aerosols are 100% soluble. The simulated ^{7}Be is subject to all the advection, mixing and convection processes consistent with the model air mass fluxes. In stratiform and convective clouds, aerosol species are transported and handled according to processes for each cloud type. Aerosol gravitational settling is also included, and fine aerosols are allowed to settle faster in the stratosphere, where the mean free path exceeds the particle radius [*Koch and Rind*, 1998]. The same turbulent exchange coefficients as those used for the model humidity are applied to ^{7}Be near the surface. The resistance-in-series scheme described in the study by *Wesely and Hicks* [1977] (derived from the Harvard GISS chemical transport model [e.g., *Chin et al.*, 1996]) is the basis for the model's dry deposition scheme. This scheme is fully coupled to the GCM processes and incorporates the GCM-assumed leaf area indices, surface types, radiation, boundary layer height and Monin-Obukhov length [*Koch et al.*, 2006].

[12] Since the SEP event took place on 20 January, we ran the simulations from 1 January through 27 February 2005, in order to capture the effects of the production spike in the weeks that followed. To simulate the conditions in January and February 2005 as realistically as possible, we used a present-day atmospheric composition and forced the model with observed sea surface temperatures and sea ice values. Also, we used NCEP/NCAR reanalysis data to "nudge" the model winds so that they more closely resemble the observed values. This is done by relaxing the horizontal wind field toward the horizontal components of the reanalysis data [*Bauer et al.*, 2004]. Because the vertical mass flux is calculated as a residual of the horizontal winds, sub-gridscale vertical movements will tend to be smoothed out. Since atmospheric ^{7}Be concentrations increase rapidly with altitude, changes associated with storm systems and other vertical mixing processes can have a significant impact on surface air concentrations. To the extent that the residual vertical motions are realistic, we expect that the ^{7}Be concentrations near the surface will be well modeled. However, errors in the reanalysis plus deviations from the input winds due to the model's internal dynamics may lead to departures from the observed situation.

[13] The spin-up to 1 January 2005 was over a 10-year period with 2004 wind conditions so that the ^{7}Be was in full equilibrium. There may therefore be small transients that we are not capturing (such as those that are a function of the solar cycle), but these are small compared with the variations due to advection which are dominant on synoptic timescales.

[14] In order to study in detail the effect of the SEP event, we performed two model runs: a "SEP" and a "no SEP" run. In both runs, ^{7}Be production varied on a daily basis, however the "SEP" run included the SEP-induced spike of ^{7}Be production on 20 January, and the "no SEP" run was performed without the spike. The model outputs the computed concentration (in ppmv: parts per million by volume) of ^{7}Be averaged over the grid box and time step. An example of the computed ^{7}Be concentration at the level of 192 mb is shown in Figure 2 for a quiet day of 12 January 2005. In order to match individual data locations and heights, we perform a 3D interpolation of the gridded output.

3. Testing the Air Mass Transport

[15] The results of the model computations were compared with the measurements for each site individually (Table 1). Most of the analyzed stations are located at low altitude, and we use the model results for the atmospheric layer with the pressure boundary of 984 mb, corresponding to about 250 m a.s.l. for the standard atmosphere. The only station situated at higher altitude is DEP33 Freiburg (1208 m a.s.l., see Table 1), for which we used results for the atmospheric layer with the 884 mb pressure boundary. For the purpose of explicit comparison, all the measured data, given originally in μBq/m^3, have been straightforwardly (1 μBq/m^3 = 2.49825×10^{-19} ppmv) translated into the units of ppmv, output by the model. We emphasize that the model results were considered exactly as yielded by the model, without any adjustment or normalization. Therefore we compare not only the relative variations but also the absolute values of the isotope's concentration in the ambient air.

[16] Comparison between the measured and modeled ^{7}Be concentrations is shown in Figures 3 and 4 for all the selected sites. First we check the results for the winter conditions (Northern hemisphere). Agreement between the

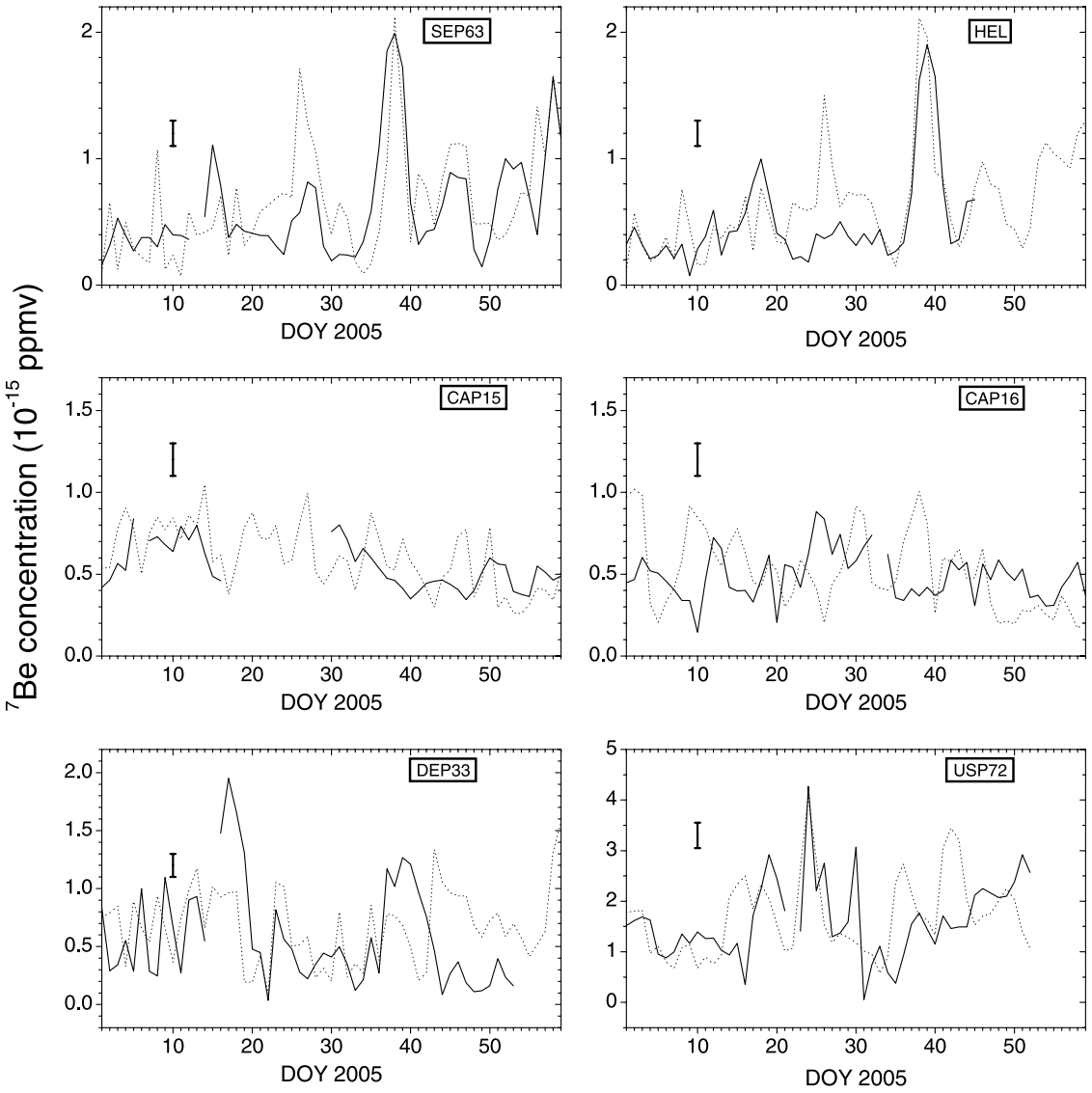

Figure 3. Measured (solid curves) and modeled (dotted curves) daily concentration of ^{7}Be in the near-ground air for the beginning of the year 2005. Each graph corresponds to a measuring site (see Table 1) in the northern hemisphere. Concentration is presented in 10^{-15} ppmv. Measurement uncertainties (shown as a thick error bar in each graph) are composed of about 7% (see section 2.1).

model and actual measurements of ^{7}Be concentration is very good for the Stockholm station (Figure 3, SEP63). The absolute value of the modeled concentration matches well with that obtained from measurements, including a relatively low level of $2-4 \times 10^{-16}$ ppmv in January and an enhancement toward late February. The main temporal features are also well reproduced: The major peak of concentration at day 38 is precisely reproduced by the model; another peak at day 26 is reproduced qualitatively, but the model overestimates its level. A small observed peak at day 14 is not reproduced by the model, which instead yields a short peak at day 8, absent in the real data; the oscillatory pattern between days 42 and 59 is fairly well reproduced. Measurements at the Helsinki station (Figure 3, HEL) are also well reproduced by the model. The baseline of the modeled concentration follows nearly perfectly that of the actual data, except for a period at day 26, when a peak (similar to that at the SEP63 station) is predicted by the model but is absent in the data. The major peak at day 39 is perfectly modeled. We note that the large enhancement of the ^{7}Be concentration in the Fennoscandic region (sites SEP63 and HEL) at day 38–39 was related to a large-scale process of intrusion and lowering of a continental air mass rich in ^{7}Be. The ^{7}Be concentration at the two Canadian sites (CAP15 and CAP16) was relatively stable during the studied period, without distinct peaks. While the overall levels and their slow variations are well reproduced by the model (nearly perfectly for the CAP15 site and reasonably well for the CAP16 site), the variations on the daily scale do not match. Long variations are reasonably well reproduced by the model for the DEP33 site until day 42, when the model and real data begin to diverge. The observed peak at day 17 does not appear in the model results. The model reproduces very well the behavior of the ^{7}Be concentration

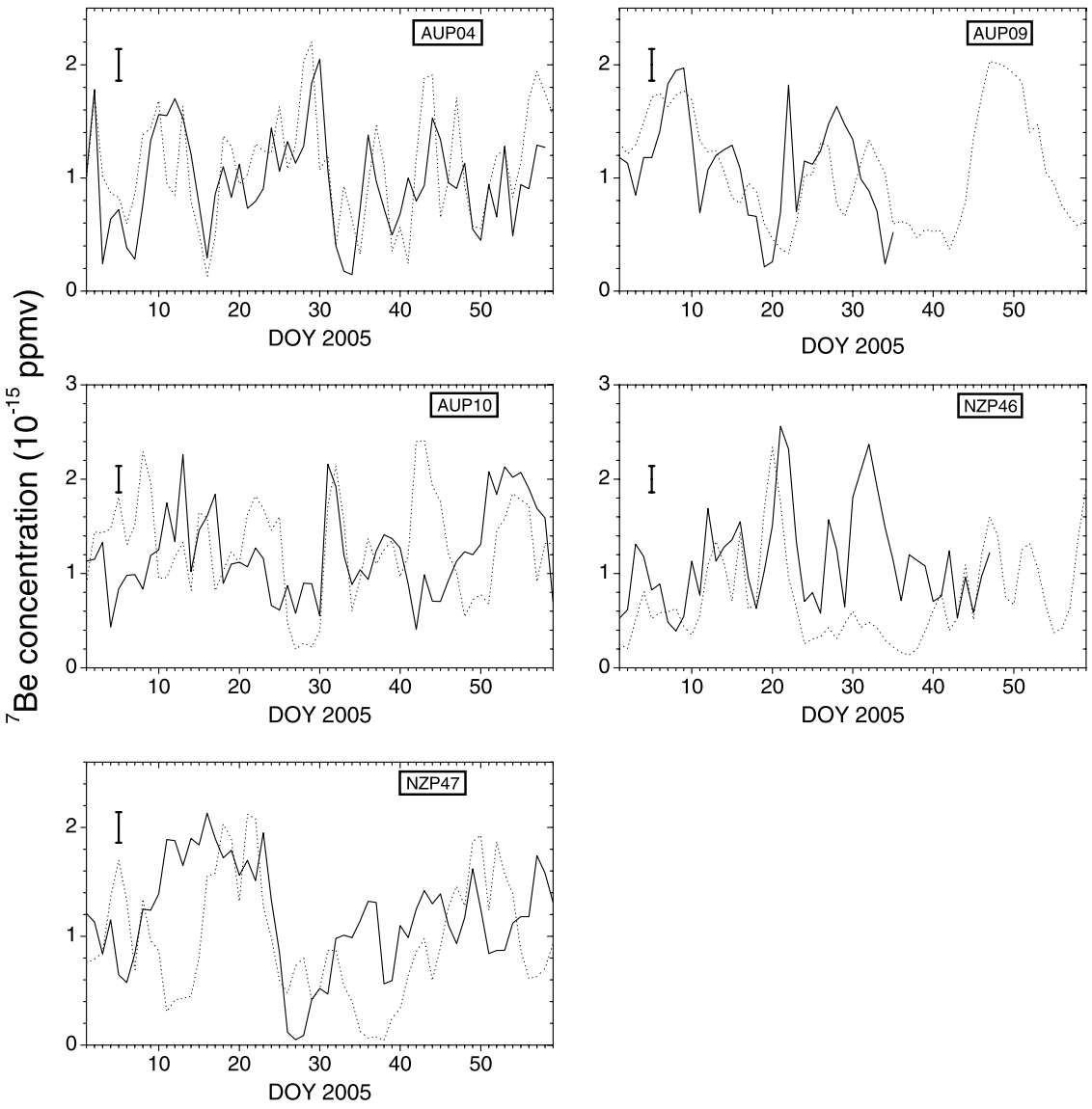

Figure 4. The same as in Figure 3 but for the southern hemisphere.

at the USP72 site, including the baseline and a peak at day 24. Some spurious peaks appear in the model results in the late part of the analyzed interval.

[17] Next we check the results for the mid-summer conditions (Southern hemisphere). The agreement between model and measurements is excellent for the AUP04 site (Figure 4), with all the features being well reproduced by the model. The temporal behavior of ^{7}Be measured at the AUP09 site is well reproduced in the main pattern (oscillations about 3 weeks in length) but some fine details are missing in the model results. The variations of ^{7}Be at the AUP10 station is more noisy. While the model reproduces the general pattern, fine details are unevenly resolved: for example, the peak at day 31 is precisely modeled, a similar peak on day 13 is not reproduced. The model also yields a spurious peak at day 42. The model precisely reproduces (with maybe a 1-day time inaccuracy) the variations at the site NZP46 before the day 25, but underestimates the isotope's concentration after that. The main pattern at the station NZP47 is captured in general by the model, but the details and the exact timing are only poorly reproduced.

[18] We also analyzed coherence between the measured and modeled concentrations of ^{7}Be. The coherence can be interpreted as localization of the correlation coefficient in the frequency domain, so that correlation is shown as a function of frequency/period, averaged over the entire time interval. We used the standard magnitude-squared coherence [*Kay*, 1988], $C_{xy}(f)$, which quantifies (between 0 and 1) the agreement between two series x and y at frequency f:

$$C_{xy}(f) = \frac{|S_{xy}(f)|^2}{S_{xx}(f)S_{yy}(f)}, \tag{2}$$

where S stands for the power spectral density of either the cross spectrum xy or the individual series x or y. The coherence is shown in Figure 5 for all the selected sites, except the gapped CAP15 and DEP33 series. One can see that short (less than 4 days) variations of the modeled ^{7}Be

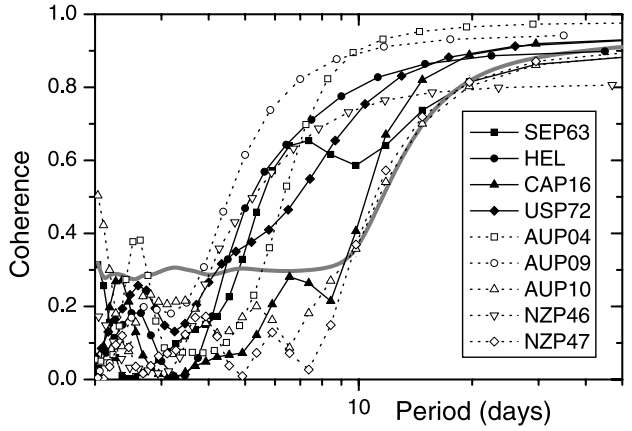

Figure 5. Coherence between measured and modeled series of ^{7}Be concentrations for the sites, as denoted in the legend. The thick gray curve depicts the 90% confidence level, estimated used the non-parametric random phase test [*Ebisuzaki*, 1997].

concentration are generally not related to the measured fluctuations, as the coherence is low and insignificant. On the other hand, all the analyzed series depict a highly significant coherence at timescales longer than 10 days. Note that, while the absolute value of coherence is high at the timescales above 20 days, the significance may be lower, because of the limited length of the series. The best results are obtained for AUP09, NZP46, SEP63 and HEL sites, where the variability is adequately modeled already at the 4-day timescale. For such sites as NZP47, AUP10 and CAP16, the model starts significantly reproducing the temporal variations only at 9- to 10-day scale. Thus all the analyzed modeled data series reproduce the temporal variability of the measured data with the significance above 90% at timescales longer than approximately a week. This timescale is associated with the synoptic weather systems at these latitudes and is a consequence of the large-scale coherence of the model to the observed sea level pressure patterns.

[19] Summarizing this comparison, we can conclude that:

[20] • The model reproduces within about 10% accuracy the overall level of the near-ground ^{7}Be concentration, which varies by an order of magnitude between (sub)polar and tropical sites. The overall level is also correctly reproduced for the mountain site DEP33 (1200 m elevation). This suggest that neither the OuluCRAC:7Be nor the GISS ModelE models make notable errors in the simulations of the ^{7}Be production rate and its large-scale transport, or that these diagnostics are not sensitive to such errors.

[21] • The slowly changing (timescales of 4 days and longer) baseline of the ^{7}Be concentration is well reproduced by the model for all the sites in both winter (Northern hemisphere) and summer (Southern hemisphere) conditions.

[22] • Most of the strong peaks in the measured ^{7}Be concentration are well reproduced by the model, in terms of both the timing and amplitude. However, some increases in concentration are not adequately reproduced by the model. The model sometimes yields short spurious peaks, as e.g., at day 26 at SEP63 and HEL sites.

[23] We can conclude that, while the model does not resolve all the small-scale dynamics in the observed air mass transport, it is pretty good in reproducing the large-scale pattern (timescales of 4 days and longer than a week), both qualitatively and quantitatively. While the model's representation of sea level pressure on monthly mean and daily timescales is similar to the observed values, the nudging scheme used in these experiments still creates small discrepancies, with better performance at high-latitude and midlatitudes than in the tropics. The fidelity of the daily fluctuations in the model are therefore limited by the discrepancies in the sea level pressure fields and the associated patterns in vertical motion. Discrepancies between the modeled and observed 7Be may also be related to the model's inability to resolve small-scale occurrences of stratosphere-troposphere exchange.

4. Effect of Solar Energetic Particles

[24] Although the enhanced production of nuclei due to SEPs in the uppermost atmosphere can be directly observed from satellites [*Phillips et al.*, 2001; *Share et al.*, 2002], the effect in the lower atmosphere needs to be studied. In order to resolve the SEP effect, we compare the results of the "SEP" and "no SEP" runs of the ^{7}Be production/transport model, which are identical to each other in all respects except for including/ignoring the additional ^{7}Be production by the SEP event on 20 January 2005 (see section 2.3). The effect of the SEP event for every location (λ, ψ), altitude (h) and time (t) is then defined as the normalized excess of the ^{7}Be concentration, calculated by the "SEP" model, C, with respect to that of the "no SEP" model, C_0:

$$R(\lambda, \psi, h, t) = \frac{C(\lambda, \psi, h, t)}{C_0(\lambda, \psi, h, t)} - 1. \quad (3)$$

[25] An example of the spatial distribution of the effect of the SEP event is shown in Figure 6 for the altitude of about 12 km (pressure level 192 mb). Figure 6a shows the SEP effect for the very day of the event and reflects only direct production of the isotope. The enhancement of the ^{7}Be concentration is quite homogeneous (about 7% at this altitude and an order of magnitude greater in the upper stratosphere) and is limited to the geomagnetic latitude above 60°. Note that this region takes the sigmoid shape because of the tilt of the geomagnetic axis with respect to the geographical axis. A spot of even higher (above 10%) concentration south of Australia corresponds to the southern (geomagnetically northern) magnetic pole and was caused by the highly anisotropic prompt component of the SEP event [*Bazilevskaya et al.*, 2008]. Next, Figure 6b shows the spatial distribution of the effect 11 days later (31 January). Here both horizontal and vertical transports are important. In the Southern hemisphere with its austral summer, the enhanced (5–6%) concentration occupies all geographical latitudes above 50 nearly uniformly with some small plumes extending to 30°. The situation in the Northern winter hemisphere is more complicated. Because of the intensive air mass transport, the enhanced concentration quickly advances to subtropical latitudes in the Far East and Pacific regions, but retreated to 50–70° latitude in the North Atlantic region.

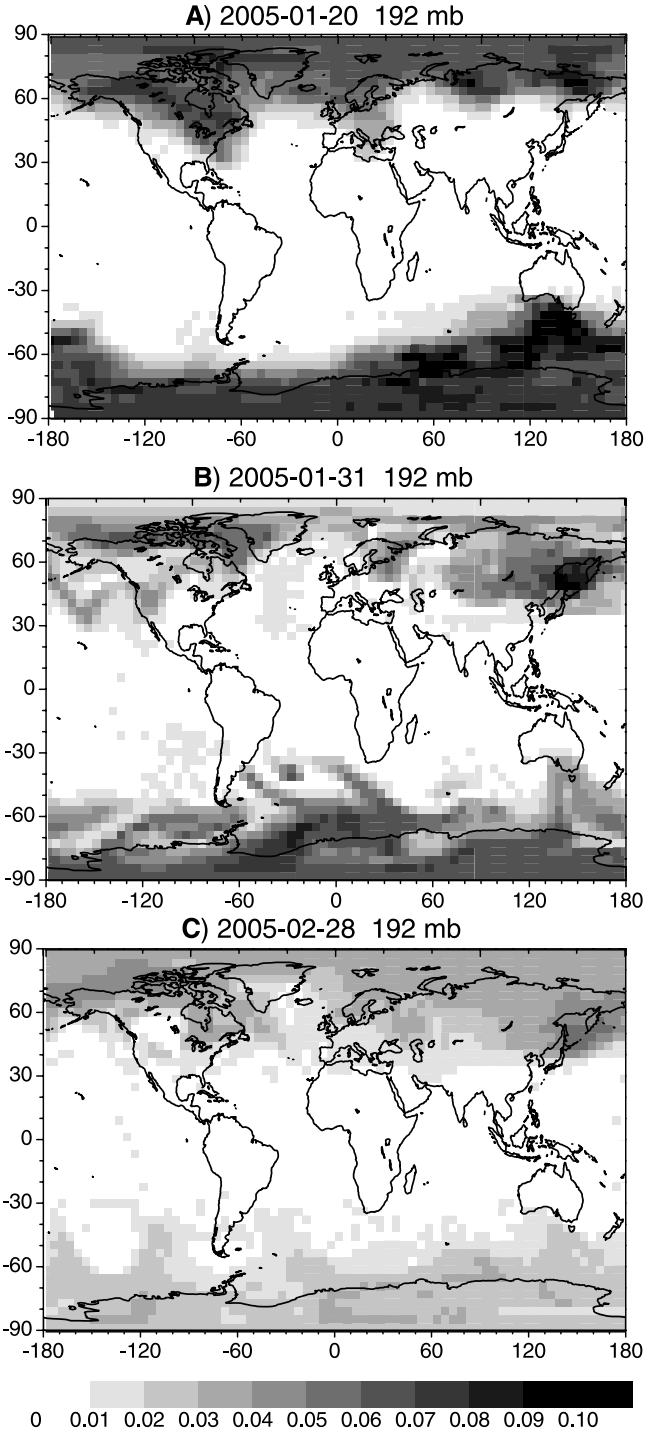

Figure 6. Spatial (geographical latitude-longitude) distribution of the computed effect (see text for definition) of SEP event of 20 January 2005, in the ^{7}Be concentration at the atmospheric level of 192 mb (about 12 km altitude). The gray scale in the bottom applies to all panels. The distribution is shown for days of (a) 20 January, (b) 31 January, and (c) 27 February.

[26] Figure 6c shows the situation 40 days after the event, when about 40% of the ^{7}Be atoms produced during the event have already decayed. The enhanced concentration (3–4% on average) occupies now all latitudes above 45° nearly homogeneously with some signatures of the zonal patterns, particularly in the southern hemisphere.

[27] In summary, the pattern of an SEP event on the ^{7}Be concentration in air is defined by the local production in the very first days after the event, after which it is dominated by the large-scale air mass transport, including vertical transport. Within a month or so, air concentrations are homogenized in the midlatitude and high latitudes (above roughly 45° latitude).

[28] We have also analyzed the time and altitude variability of the SEP effect for the high-latitude (60–64° N) zonal mean, where the expected effect is high (Figure 7). While the absolute production of ^{7}Be peaks around 15–20 km, the SEP effect starts dominating over the GCR production above 20 km altitude (Figure 1). Accordingly, the immediate SEP effect can be directly observed only in the upper stratosphere. The modeled effect of SEP event is very strong (two orders of magnitude greater than the daily GCR-related production) and instantaneous at the altitude above 50 km. The additionally produced ^{7}Be does not stay at this atmospheric level but moves down as shown in the figure, descending to 40–50 km within a week. After a fortnight there is no indication of the enhanced ^{7}Be concentration at these altitude.

[29] The ^{7}Be concentration enhanced by an order of magnitude is expected in the middle troposphere (about 25–30 km). While the immediate effect of SEP (on 20 January) was of a factor of 14 at 30 km altitude, the enhanced concentrations stays nearly constant at the level of enhancement by a factor of 10–20 for about a month due to the steady advection of ^{7}Be from upper layers. The effect of the SEP event rapidly decreases with lowering altitude, being factors of 3, 0.25 and 0.07 at about 25 km, 20 km and 14 km, respectively. However, because of the redistribution of the produced isotope (in particular by the vertical motion), the enhanced concentration persists for weeks. The modeled SEP effect is strong enough to be directly observed in the stratosphere, but it is weak in the troposphere, at the level of 2–3%, and is mostly secondary (i.e., due to the downward transport of the additionally produced ^{7}Be), with the direct effect not exceeding 2%, which is smaller than the measurement uncertainties. Some slight enhancements might be expected during a couple of weeks after the event, but these cannot be distinguished over the background variations of several percent (see section 2.1).

[30] Summarizing this analysis we can conclude that the instantaneous direct effect of the SEP event is strongest in the upper stratosphere, with concentrations of ^{7}Be increasing by two orders of magnitude due to the enhanced in-site production. In the lower stratosphere and troposphere, the effect is twofold: a peak of ^{7}Be concentration on the first day is the result of the direct production effect, and enhanced concentration extends for months because of the descent of ^{7}Be produced largely in higher atmospheric layers.

[31] The expected effect (2–3%) of an extreme SEP event, as predicted by the model, is apparently too small to be detected at the near-ground data analyzed here, in agreement with an earlier fragmentary study [*Yoshimori*, 2005b]. Direct measurements in the stratosphere, where the ^{7}Be concentration is expected to be enhanced by a factor of 2–10 during the weeks following the event, would make it possible to test the model results directly. However, we are

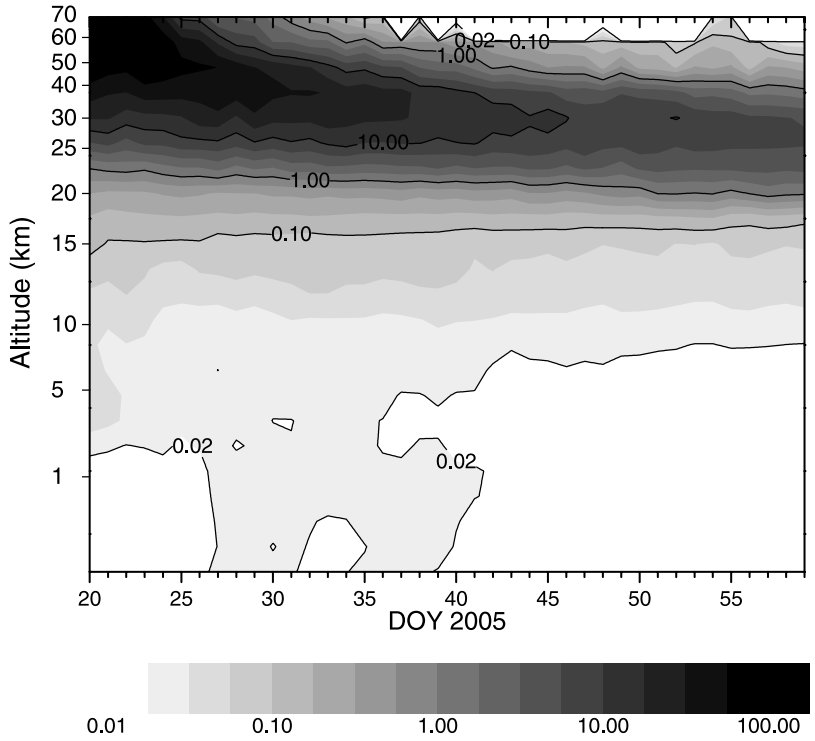

Figure 7. Effect (see text for definition) of solar energetic particles from the SEP event of 20 January 2005 on the computed ^{7}Be concentration in the atmosphere in subpolar zonal mean (60–64°N latitude, averaged over all longitudes).

not aware of such measurements performed during January or February 2005.

5. Discussion and Conclusions

[32] We presented the results of testing of an atmospheric GCM model using the cosmogenic isotope ^{7}Be as a tracer of air mass transport in the Earth's atmosphere. A combination of a numerical model of ^{7}Be production and transport has been developed, using the GISS ModelE atmospheric circulation model, where in situ production of ^{7}Be by cosmic rays is included explicitly as computed by the OuluCRAC:7Be model. The combined model allows us to trace the air mass transport by means of the ^{7}Be concentration in full 3D on daily timescales. In order to evaluate the model, its results were directly compared with routine daily measurements of the ^{7}Be concentration in near-ground air performed by radiation safety authorities in different countries covering the latitudinal range from tropics to polar regions (see Table 1). The model reproduces well both the overall level of ^{7}Be concentration in the near-ground air, which varies by an order of magnitude between different monitoring stations, and also the large-scale variations in air concentration, including, e.g., a pronounced peak on 6–10 February in Fennoscandian sites SEP63 and HEL.

[33] We note that while the results of the OuluCRAC:7Be production model are in good agreement with semi-empirical models [*Lal and Peters*, 1967; *Nagai et al.*, 2000; *O'Brien*, 1979] and fragmentary in situ measurements (see section 3 in the study by *Usoskin and Kovaltsov* [2008]), some numerical models [*Masarik and Beer*, 1999; *Webber et al.*, 2007] may somewhat underestimate the production as mentioned by *Kollár et al.* [2000] and *Heikkilä et al.* [2008]. The Monte-Carlo core of the OuluCRAC:7BE model is essentially the same as that of the OuluCRAC:CRII model [*Usoskin and Kovaltsov*, 2006], which computes the cosmic ray-induced ionization in the atmosphere. The latter has been verified, by comparison with observational data and independent model simulations, to correctly simulate the atmospheric cascade within 10% accuracy [*Bazilevskaya et al.*, 2008; *Usoskin et al.*, 2009], which confirms the correctness of the cascade core simulations by the OuluCRAC model. The overall agreement with measurements obtained here implies that our OuluCRAC:7Be model correctly simulates the production of ^{7}Be, including the overall normalization.

[34] We also found that our combined model adequately reproduces transport of air masses on large scales (timescales of 4 days or longer). However, details at shorter timescales and on sub-synoptic length scales are unevenly described by the model: while some variations are precisely reproduced (e.g., for the APU04 site), some other are either not reproduced (e.g., a peak on 18 January at DEP33 station) or over-reproduced (e.g., a short peak on 26 January at the SEP63 site) by the model. Short-term fluctuations at the diurnal scale are typically not reproduced by the model. This suggests that the combined model simulates correctly the large-scale atmospheric dynamics but does not possess sufficient precision to distinguish small-scale effects. This is probably related to the nudging scheme used in these model runs (section 2.3). The present comparison is limited to the lowest atmospheric layer, since the routine measurements of ^{7}Be concentration are only performed near the ground. However, since the isotope is mostly produced in the upper

atmospheric layers, the present results imply that the model also works correctly for higher altitudes, at least in the troposphere. For that layer, the model succeeds in matching the magnitude of the observed ^{7}Be concentrations, as well as the range of variability and the general trends at the different northern hemisphere and southern hemisphere locations.

[35] We have also studied the effect of a severe solar energetic particle event on ^{7}Be in the atmosphere. The severe SEP event of 20 January 2005, resulted in an instant "injection" of ^{7}Be atoms into the atmosphere. The simulations suggest that the effect of the SEP event on ^{7}Be concentration is twofold. The instantaneous effect of the enhanced local production due to solar particles is limited to polar regions but occupies the entire atmospheric column, varying from two to three orders of magnitude in the upper stratosphere to a few percent in the lower troposphere. This immediate effect dominates in the upper atmosphere, from where ^{7}Be produced by the SEP event descends to the stratosphere within several days. On the other hand, the enhanced concentration of ^{7}Be in stratosphere and troposphere is prolonged for month(s), mostly because of the downward transport of ^{7}Be from upper atmospheric layers. The effect of notably enhanced ^{7}Be concentration extends from (geomagnetic) polar regions to occupy the entire midlatitude and high latitudes, with a clear zonal structure in the Southern hemisphere (local summer). Unfortunately, the expected effect of the SEP event is too small (about 2%) at the ground level to be securely detected in the measured data. Direct airborne measurements of ^{7}Be concentration in the upper troposphere or stratosphere, even performed several weeks after a strong SEP event, could provide extremely valuable information for direct tests of air circulation models.

[36] In conclusion, we have developed and directly verified a novel combined model of production and transport of the cosmogenic tracer ^{7}Be in the atmosphere. We have shown that synoptic variations in ^{7}Be can be captured by a nudged GCM including aerosol tracers. Further analysis of the causes of these variations and more detailed studies of stratosphere/troposphere interactions may allow more fundamental tests of the model leading to better understanding of the air mass transport processes.

[37] **Acknowledgments.** We gratefully acknowledge CTBTO for funding, building, and maintaining the monitoring station network. We thank the Finnish National Data Centre for providing access to the ^{7}Be data in the FiNDC database. We also acknowledge national authorities in United States, Canada, Sweden, Germany, Australia, and New Zealand for providing the necessary permissions for use of monitoring data in scientific studies. Climate modeling at GISS is supported by NASA Modeling, Analysis and Prediction program. C.F. also acknowledges support from the US National Science Foundation through a Fellowship in the IGERT Joint Program in Applied Mathematics and Earth and Environmental Sciences at Columbia University. Supports from the Academy of Finland and Suomalainen Tiedeakatemia (Väisälä Foundation) are acknowledged. G.A.K. was partly supported by the Program of Presidium RAS N16-3-5.4.

References

Aarnio, P. A., et al. (2008), LINSSI: Database for gamma-ray spectrometry, *J. Radioanal. Nucl. Chem.*, *276*, 631–663.

Ala-Heikkilä, J. (2008), *Analysis Methods for Airborne Radioactivity*, *TKK-DISS-2491*, Helsinki Univ. of Technology, Helsinki, Finland.

Aldahan, A., G. Possnert, and I. Vintersved (2001), Atmospheric interactions at northern high latitudes from weekly Be-isotopes in surface air, *Appl. Radiat. Isot.*, *54*, 345–353.

Bauer, S., Y. Balkanski, M. Schulz, D. Hauglustaine, and F. Dentener (2004), Global modeling of heterogeneous chemistry on mineral aerosol surfaces: Influence on tropospheric ozone chemistry and comparison to observations, *J. Geophys. Res.*, *109*, D02304, doi:10.1029/2003JD003868.

Bazilevskaya, G. A., et al. (2008), Cosmic ray induced ion production in the atmosphere, *Space Sci. Rev.*, *137*, 149–173.

Bratt, S. (2001), The International Data Centre of the Comprehensive-Nuclear Test Ban Treaty: Vision and progress, *Kerntechnik*, *66*, 134–142.

Chin, M., D. J. Jacob, G. M. Gardner, M. S. Foreman-Flower, P. A. Spiro, and D. L. Savoie (1996), A global three-dimensional model of tropospheric sulfate, *J. Geophys. Res.*, *101*, 18,667–18,690.

Dorman, L. (2004), *Cosmic Rays in the Earth's Atmosphere and Underground*, Springer, Dordrecht.

Ebisuzaki, W. (1997), A method to estimate the statistical significance of a correlation when the data are serially correlated, *J. Clim.*, *10*, 2147–2153.

Ellison, D. C., and R. Ramaty (1985), Shock acceleration of electrons and ions in solar flares, *Astrophys. J.*, *298*, 400–408.

Fassò, A., A. Ferrari, J. Ranft, and P. Sala (2001), Fluka: Status and prospective of hadronic applications, in *Proc. Monte Carlo 2000 Conf.*, edited by A. Kling et al., pp. 955–960, Springer, Berlin.

Field, C. V., G. A. Schmidt, D. Koch, and C. Salyk (2006), Modeling production and climate-related impacts on ^{10}Be concentration in ice cores, *J. Geophys. Res.*, *111*, D15107, doi:10.1029/2005JD006410.

Heck, D., J. Knapp, J. Capdevielle, G. Schatz, and T. Thouw (1998), *CORSIKA: A Monte Carlo Code to Simulate Extensive Air Showers*, FZKA 6019, Forschungszentrum, Karlsruhe.

Heikkilä, U., J. Beer, and J. Feichter (2008), Modeling cosmogenic radionuclides ^{10}Be and ^{7}Be during the Maunder Minimum using the ECHAM5-HAM General Circulation Model, *Atmos. Chem. Phys.*, *8*, 2797–2809.

IPCC (2007), *Climate Change 2007—The Physical Science Basis, Contribution of Working Group I to the Fourth Assessment Report of the IPCC*, Cambridge Univ. Press, New York.

Jordan, C. E., J. E. Dibb, and R. C. Finkel (2003), ^{10}Be/^{7}Be tracer of atmospheric transport and stratosphere-troposphere exchange, *J. Geophys. Res.*, *108*(D8), 4234, doi:10.1029/2002JD002395.

Kay, S. (1988), *Modern Spectral Estimation: Theory and Application*, Prentice Hall, New Jersey.

Koch, D., G. A. Schmidt, and C. Field (2006), Sulfur, sea salt and radionuclide aerosols in GISS ModelE, *J. Geophys. Res.*, *111*, D06206, doi:10.1029/2004JD005550.

Koch, D. M., and D. Rind (1998), Beryllium 10/beryllium 7 as a tracer of stratospheric transport, *J. Geophys. Res.*, *103*, 3907–3917.

Koch, D. M., D. J. Jacob, and W. C. Graustein (1996), Vertical transport of tropospheric aerosols as indicated by ^{7}Be and ^{210}Pb in a chemical tracer model, *J. Geophys. Res.*, *101*, 18,651–18,666.

Kollár, D., I. Leya, J. Masarik, and R. Michel (2000), Calculation of cosmogenic nuclide production rates in the earth atmosphere and in terrestrial surface rocks using improved neutron cross sections, *Meteorit. Planet. Sci. Suppl.*, *35*, A90–A91.

Kulan, A., A. Aldahan, G. Possnert, and I. Vintersved (2006), Distribution of ^{7}Be in surface air of Europe, *Atmos. Environ.*, *40*, 3855–3868.

Lal, D., and B. Peters (1962), Cosmic ray produced isotopes and their application to problems in geophysics, in *Progress in Elementary Particle and Cosmic Ray Physics*, vol. 6, edited by J. Wilson and S. Wouthuysen, p. 244, North Holland, Amsterdam.

Lal, D., and B. Peters (1967), Cosmic ray produced radioactivity on the earth, in *Handbuch der Physik*, vol. 46/2, edited by K. Sittle, pp. 551–612, Springer, Berlin.

Liu, H., D. J. Jacob, I. Bey, and R. M. Yantosca (2001), Constraints from ^{210}Pb and ^{7}Be on wet deposition and transport in a global three-dimensional chemical tracer model driven by assimilated meteorological fields, *J. Geophys. Res.*, *106*, 12,109–12,128.

Lockwood, J. A., H. Debrunner, E. O. Flueckiger, and H. Graedel (1990), Proton energy spectra at the sun in the solar cosmic-ray events on 1978 May 7 and 1984 February 16, *Astrophys. J.*, *355*, 287–294.

Masarik, J., and J. Beer (1999), Simulation of particle fluxes and cosmogenic nuclide production in the Earth's atmosphere, *J. Geophys. Res.*, *104*, 12,099–12,111.

Mathews, S., and J. Schulze (2001), The radionuclide monitoring system of the Comprehensive-Nuclear Test Ban Treaty Organisation: From sample to product, *Kerntechnik*, *66*, 102–112.

Medici, F. (2001), Particulate sampling in the IMS radionuclide network of the Comprehensive-Nuclear Test Ban Treaty, *Kerntechnik*, *66*, 121–125.

Mewaldt, R. A. (2006), Solar energetic particle composition, energy spectra, and space weather, *Space Sci. Rev.*, *124*, 303–316.

Mironova, I. A., D. Desorgher, I. G. Usoskin, E. Flückiger, and R. Bütikofer (2008), Variations of aerosol optical properties during the extreme solar event in January 2005, *Geophys. Res. Lett.*, *35*, L18160, doi:10.1029/2008GL035120.

Nagai, H., W. Tada, and T. Kobayashi (2000), Production rates of ^{7}Be and ^{10}Be in the atmosphere, *Nucl. Instrum. Methods Phys. Res. Sect. B*, *172*, 796–801.

O'Brien, K. (1979), Secular variations in the production of cosmogenic isotopes in the earth's atmosphere, *J. Geophys. Res.*, *84*, 423–431.

Phillips, G., et al. (2001), Correlation of upper-atmospheric ^{7}Be with solar energetic particle events, *Geophys. Res. Lett.*, *28*, 939–942.

Plainaki, C., A. Belov, E. Eroshenko, H. Mavromichalaki, and V. Yanke (2007), Modeling ground level enhancements: Event of 20 January 2005, *J. Geophys. Res.*, *112*, A04102, doi:10.1029/2006JA011926.

Raisbeck, G. M., F. Yiou, M. Fruneau, J. M. Loiseaux, M. Lieuvin, and J. C. Ravel (1981), Cosmogenic Be-10/Be-7 as a probe of atmospheric transport processes, *Geophys. Res. Lett.*, *8*, 1015–1018.

Rind, D., J. Lerner, K. Shah, and R. Suozzo (1999), Use of on-line tracers as a diagnostic tool in general circulation model development. 2: Transport between the troposphere and stratosphere, *J. Geophys. Res.*, *104*, 9151–9168.

Rind, D., J. Lerner, J. Jonas, and C. McLinden (2007), Effects of resolution and model physics on tracer transports in the NASA Goddard Institute for Space Studies general circulation models, *J. Geophys. Res.*, *112*, D09315, doi:10.1029/2006JD007476.

Schmidt, G. A., et al. (2006), Present day atmospheric simulations using GISS ModelE: Comparison to in-situ, satellite and reanalysis data, *J. Clim.*, *19*, 153–192.

Share, G. H., R. J. Murphy, B. R. Dennis, R. A. Schwartz, A. K. Tolbert, R. P. Lin, and D. M. Smith (2002), RHESSI observation of atmospheric gamma rays from impact of solar energetic particles on 21 April 2002, *Solar Phys.*, *210*, 357–372.

Shindell, D. T., G. Faluvegi, N. Unger, E. Aguilar, G. A. Schmidt, D. M. Koch, S. E. Bauer, and R. L. Miller (2006), Simulations of preindustrial, present-day, and 2100 conditions in the NASA GISS composition and climate model G-PUCCINI, *Atmos. Chem. Phys.*, *6*, 4427–4459.

Stoker, P. H. (1995), Relativistic solar proton events, *Space Sci. Rev.*, *73*, 327–385.

Ungar, K., et al. (2007), Automation of analysis of airborne radionuclides observed at Canadian CTBT radiological networks using LINSSI, *J. Radioanal. Nucl. Chem.*, *272*, 285–291.

Usoskin, I. G., and G. A. Kovaltsov (2006), Cosmic ray induced ionization in the atmosphere: Full modeling and practical applications, *J. Geophys. Res.*, *111*, D21206, doi:10.1029/2006JD007150.

Usoskin, I. G., and G. A. Kovaltsov (2008), Production of cosmogenic ^{7}Be isotope in the atmosphere: Full 3-D modeling, *J. Geophys. Res.*, *113*, D12107, doi:10.1029/2007JD009725.

Usoskin, I. G., K. Alanko-Huotari, G. A. Kovaltsov, and K. Mursula (2005), Heliospheric modulation of cosmic rays: Monthly reconstruction for 1951–2004, *J. Geophys. Res.*, *110*, A12108, doi:10.1029/2006JA011250.

Usoskin, I. G., L. Desorgher, P. Velinov, M. Storini, E. O. Flückiger, R. Bütikofer, and G. A. Kovaltsov (2009), Ionization of the earth's atmosphere by solar and galactic cosmic rays, *Acta Geophys.*, *57*, 88–101.

Webber, W. R., P. R. Higbie, and K. G. McCracken (2007), Production of the cosmogenic isotopes ^{3}H, ^{7}Be, ^{10}Be, and ^{36}Cl in the Earth's atmosphere by solar and galactic cosmic rays, *J. Geophys. Res.*, *112*, A10106, doi:10.1029/2007JA012499.

Wesely, M. L., and B. B. Hicks (1977), Some factors that affect the deposition rates of sulfur dioxide and similar gases on vegetation, *J. Air Pollut. Control Assoc.*, *27*, 1110–1116.

Yoshimori, M. (2005a), Beryllium 7 radionucleide as a tracer of vertical air mass transport in the troposphere, *Adv. Space Res.*, *36*, 828–832.

Yoshimori, M. (2005b), Production and behavior of beryllium 7 radionuclide in the upper atmosphere, *Adv. Space Res.*, *36*, 922–926.

A. Aldahan, Department of Earth Sciences, University of Uppsala, Villavägen 16, SE-752 36 Uppsala, Sweden.

C. V. Field and G. A. Schmidt, NASA GISS, 2880 Broadway, New York, NY 10025, USA.

G. A. Kovaltsov, Ioffe Physical-Technical Institute, Politekhnicheskaya 26, RU-194021 St. Petersburg, Russia.

A.-P. Leppänen, Regional Laboratory in Northern Finland, STUK, Louhikkotie 28, FIN-96500 Rovaniemi, Finland.

G. Possnert, Tandem Laboratory, University of Uppsala, Villavägen 16, SE-752 36 Uppsala, Sweden.

R. K. Ungar, Radiation Protection Bureau of Health Canada, 775 Brookfield Road, AL6302D1, Ottawa, ON K1A 1C1, Canada.

I. G. Usoskin, Sodankylä Geophysical Observatory (Oulu unit), University of Oulu, P.O. Box 3000, FIN-90014 Oulu, Finland. (ilya.usoskin@oulu.fi)